Arab J Sci Eng (2017) 42:4157–4168
DOI 10.1007/s13369-017-2571-6

RESEARCH ARTICLE - CIVIL ENGINEERING

Evaluation on Effectiveness of Cold-Formed Steel Column with Various Types of Edge Stiffener

P. Manikandan[1] · G. Aruna[1] · S. Balaji[2] · S. Sukumar[3] · M. Sivakumar[4]

Received: 7 July 2016 / Accepted: 8 May 2017 / Published online: 31 May 2017

Abstract In this study, four series of cold formed steel channel columns with different types of edge stiffeners is analyzed under pinned end conditions subjected to axial compression. The selected cross-sectional profiles are met with the interactive failure modes. The cross-sectional dimensions are satisfied the pre-qualified section properties of cold-formed steel structures. Test results are simulated with finite element analysis software using ANSYS, and good agreement has been achieved. After the validation of the proposed numerical model, the effect of variation of thickness, yield stress and overall slenderness in the strength and behaviour of the section are carried out. Interaction of distortional and flexural buckling is the governing failure modes of the column section. All the findings of FEA are compared with the Direct Strength Specification for cold-formed steel structures, and the strength of the member is also determined by using the modified equations from the literature. Based on the results, a new design equation is proposed, and also it is validated by the results available from the literature.

✉ P. Manikandan
lp_mani@yahoo.com

S. Balaji
er.sbalaji@yahoo.co.in

S. Sukumar
sukumar_237@yahoo.co.in

1 Centre for Structural Engineering research, Department of Civil Engineering, Sona College of Technology, Salem, Tamil Nadu, India

2 Kongu Engineering College, Erode Dt, Tamil Nadu, India

3 Department of Civil Engineering, Paavai Group of Institution, Namakkal Dt, Tamil Nadu, India

4 Vishwa Infrastructures and Services Pvt. Ltd., Ahmadabad, India

Keywords Cold-formed steel · Distortional buckling · Edge stiffener · Flexural buckling · Slenderness ratio

List of symbols

A	Cross-sectional area
P_{cre}	Critical elastic column buckling load in flexural buckling/flexural–torsional/torsional
P_{crl}	Critical elastic local column buckling
P_{crd}	Critical elastic distortional column buckling load
d	Depth of the channel section
$P_{d,\ DSM}$	Design strength calculated from the direct strength method
P_{EXP}	Experimental ultimate load
r_{min}	Least radius of gyration
$P_{n,\ DSM}$	Nominal strength calculated from the direct strength method
$P_{n,\ ANB}$	Nominal strength calculated from the design rules in Anbarasu et al. [23]
P_{nl}	Nominal strength for local buckling
P_{nd}	Nominal strength for distortional buckling
P_{ne}	Nominal strength for flexural–torsional buckling
$P_{n,\ Pro}$	Proposed design rules for the direct strength method
$d1$	Size of the edge stiffener
$d2$	Size of the return lip
t	Thickness of the channel section
P_{ANSYS}	Ultimate load calculated from the FE analysis
f_y	Yield stress of the material
E	Young's modulus
f_U	Ultimate stress of the material
λ	Overall slenderness ratio of the column

1 Introduction

Applications of cold-formed steel structures are increasing all over the world in building construction and automobile industry. The open cold-formed steel sections are failed by either local, distortional or Euler buckling. However, the interactive failure is more complex for designers. A simple lipped channel column with edge stiffener is more familiar with the construction industry. From the literature Wang et al. [1], it is found that the edge stiffeners can reduce effectively the rotational capacity of the flanges and improve the capacity of members. Though many studies are pertaining simple lipped channel column with upright and complex edge stiffener, the results of channels with complex edge stiffener are scattered. Hence, in this study, the effect of cross-sectional dimension, variation of yield stress and overall slenderness ratios in strength and behaviour of channel columns with complex edge stiffener are discussed.

A brief review of literature on the strength and behaviour of cold-formed steel channel column with different types of edge stiffeners which is related to this research work is presented here. A lot of experimental investigations have been undertaken on the behaviour of lipped channel column with simple edge stiffeners by Batista [2]. They developed the buckling design curve for stiffened and unstiffened long-channel column based on the Brazilian and European specification for steel construction. Young and Rasmussen [3] were taking up the study of the design lipped channel column under fixed-end condition. Young and Hancock [4] conducted a experimental study on the behaviour of cold-formed steel channel section with inward and outward inclined edge stiffeners under axial compression. The similar study was numerically verified by Young [5]. It was observed that North American Specifications provide unconservative results for the section with outward stiffener. To evaluate more accurate results for the local buckling strength of stub lipped channel column, a new design equation was suggested by Anil Kumar and Kalyanaraman [6]. Test programmes on plain channel subjected to local and coupled local–flexural instabilities were discussed by Ungermann et al. [7]. Very recently, Ananthi et al. [8] did an experimental and numerical investigation of strength and behaviour of unlipped channel columns with fixed ends. The North American Specifications for cold-formed steel structures were provided slightly unconservative results; however, for predicting the accurate results, a modification factor was proposed.

As per the DSM specifications, the design strength of the column is the least of flexural, local and distortional buckling. To improve the design guidelines of DSM specification for interactive failure modes, Young and Yan [9], Becque and Rasmussen [10], Silvestre et al. [11], Dinis et al. [12], Silvestre et al. [13], Loughlan et al. [14] discussed the local/distortional and flexural–buckling interactions of plain lipped channel columns. The effective width concept is tedious for complex cross section. Hence, a simple new design methodology (direct strength method) was developed by Schafer and Peköz [15]. Schafer [16,17] also gave the guidelines for geometric limits and validity of the developed formula for cross sections, including simple lipped channel with and without web stiffeners, Z section, hat section, and rack upright section. Continuation of this research, Yan and Young [18] conducted a study on the behaviour of cold-formed steel columns with complex edge stiffener and also evaluated the effectiveness of the DSM specifications.

In this study, a series of cold-formed steel channel column with different types of edge stiffeners is analysed under axial compression. The selected cross-sectional profile is met with the interactive failure modes. Test results are then simulated by finite element analysis using ANSYS software package, and good conformity has been achieved. Following the validation, effects of variation of thickness, overall slenderness and yield stress are discussed. All the findings from FEA are compared with the Direct Strength Specification (DSM) for cold-formed steel structures. A suitable design recommendation is stated to DSM for the cold-formed steel channel column with complex edge stiffener. The efficiency of the proposed model is verified against the test results available in the literature [18].

2 Experimental Program

2.1 Test Program

A total of six specimens with four types of sections are tested under axial compressive loading, including a simple channel column (Fig. 1a, called SC section), a simple channel column with inclined edge stiffener (Fig. 1b, called SC-I section), a simple channel column with upright edge stiffener (Fig. 1c, called SC-U section) and simple channel column with complex edge stiffener (Fig. 1d, called SC-C section).

2.2 Test Specimens

A selected cross-sectional profile with defined nomenclature is presented in Fig. 1, and details of section geometries are presented in Table 1. The geometrical sizes below are defined by surface outline. The entire test specimens are having same cross-sectional area with the nominal height of the web (d) is 130 mm, the overall nominal width of the flange (B) is 85 mm, size of the lip ($d1$) is 15 mm and size of the rear lip ($d2$) is 15 mm. The nominal width of the flange (b) for sections SC-I and SC-U is 70 mm, whereas the nominal width of the flange (b) for section SC-C is 55 mm. In these tests, three overall slenderness ratios (λ) are selected. The first column of Table 1 is the specimen identifications, which is defined

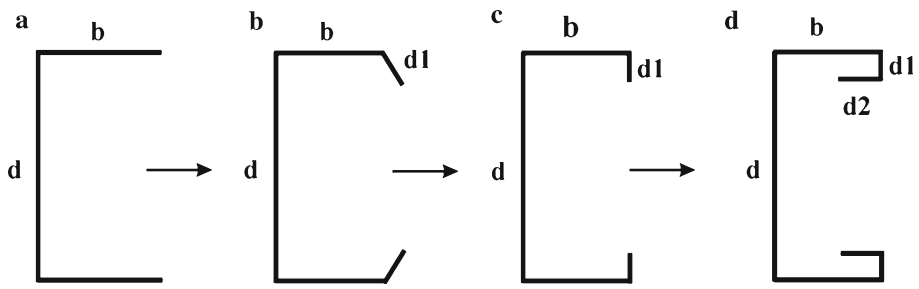

Fig. 1 Cross-sectional geometries

Table 1 Details of section geometries

Specimen ID	Section dimension (mm)					$\lambda = L/r_{min}$
	d	$b1$	$d1$	$d2$	t	
SC-λ-F270	130	85	–	–	1.6	50
SC-I-λ-F270	130	70	15	–	1.6	50
SC-U-λ-F270	130	70	15	–	1.6	30
SC-U-λ-F270	130	70	15	–	1.6	40
SC-U-λ-F270	130	70	15	–	1.6	50
SC-C1-λ-F270	130	55	15	15	1.6	50
SC-C2-λ-F270	50	50	16	14	1.6	20–120
SC-C2-λ-F350	50	50	16	14	1.6	20–120
SC-C2-λ-F550	50	50	16	14	1.6	20–120
SC-C3-λ-F270	58	42	13	17	1.6	20–120

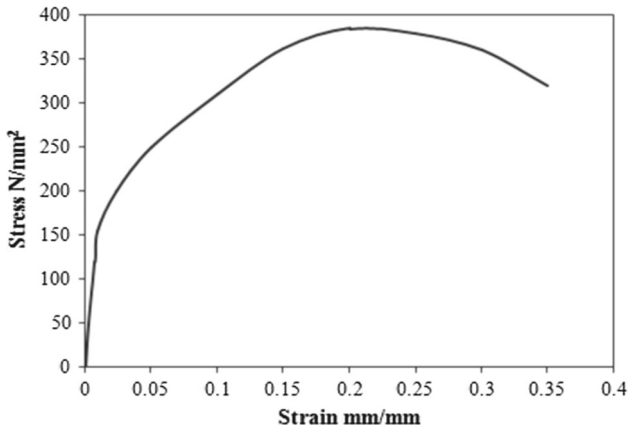

Fig. 2 Stress–strain curve

as follows: SC, SC-I, SC-U and SC-C referred to the four types of cross sections, respectively; Letter λ and the number followed by referring to the slenderness of the specimen; the last letter *F* and the number followed by referring to the yield stress of the material.

2.3 Material Properties

The tensile coupon tests are carried out as per IS 1608-2005 (Part-1). Stress–strain curve and coupons are shown in Figs. 2 and 3 respectively. Because the material tests did not display

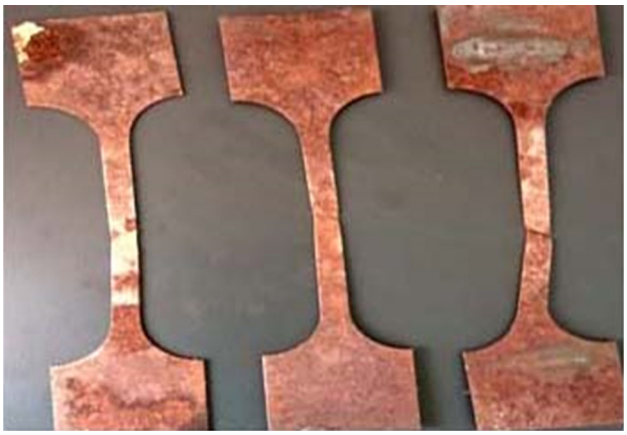

Fig. 3 Sample of the coupons

a sharp yield, the yield stress was determined by the 0.2% offset method. Material properties are listed in Table 2.

2.4 Test Set-up

The 400-kN capacity hydraulic ram is used for applying the axial compressive load. For applying uniform load and support conditions over the entire cross section, the 8-mm thickness end plates are milled flat and welded on both ends of the specimens. All the columns are tested under pin-ended boundary condition. At each end of the column, rubber gaskets are positioned to facilitate the pinned boundary condition at the supports [19,20]. A specimen is tested with a self-supported loading frame, and loads are applied by using the calibrated hydraulic ram. The ultimate load is measured with the help of load cell, and LVDT is used to measure the axial shortening of the cross section. The test set-up is displayed in Fig. 4.

3 Finite Element Modelling

In order to examine the strength and structural behaviour of the proposed column section over the different slenderness ranges, a finite element model is established by using a commercial finite element software package ANSYS. The FE model is based on the centre line dimensions of the cross

Table 2 Details of material properties

S. no.	Specimen ID	E (MPa)	f_y (MPa)	f_U (MPa)	% Elongation
1	SC-λ50- F270	2.01	268	375	19
2	SC-I-λ50- F270	2.20	269	374	20
3	SC-U-λ30- F270	2.06	271	393	16
4	SC-U-λ40- F270	2.05	277	416	25
5	SC-U-λ50- F270	2.20	274	384	21
6	SC-C1-λ50- F270	2.11	269	385	24

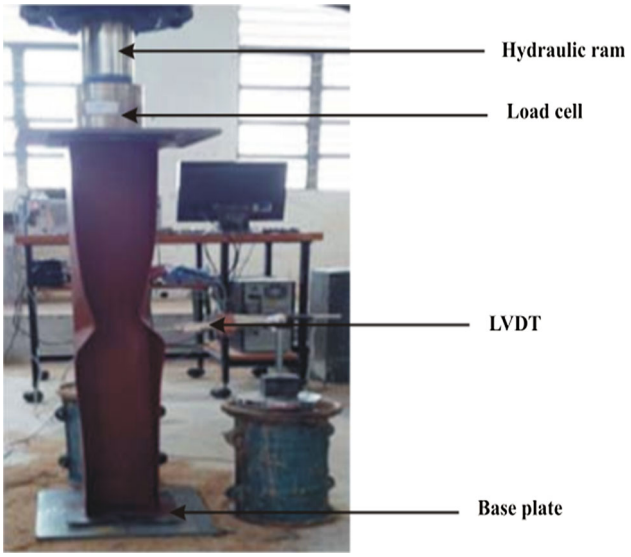

Fig. 4 Test set-up

section, and the highly efficient four-node shell element 181 is employed to generate the FE model. Through the convergence study, a uniform mesh size of 10 × 10 mm is used in the model (aspect ratios nearly equal to 1.0), and appropriate mesh size of 100 mm^2 is chosen for this study.

The influence of rounded corners with internal radius $r \leq 5t$ and $r \leq 0.15w$ ($r \leq 5 \times 1.6 = 8$ mm, $0.15 \times 85 = 12.75$ mm) on section properties can be neglected based on ENV (2006). All the specimens are fabricated using the latest computerized cutting and sharp folding press-braking machine. The sharp cutting edges provide right angular edge only. The residual stresses are not measured because both the flexural and membrane residual stresses tend to be insignificant compared with the yield stress in specimens made using the press-braking process [18]. Based on that, the effect of residual stress and cold-forming process has been ignored in the FE model.

The end conditions of the columns are pin ended [at loaded end Ux = Uy = Rz = 0 and unloaded end Ux = Uy = Uz = Rz = 0, [21]]. To ensure the axial loading condition, all the support reaction and load are applied at the CG of the

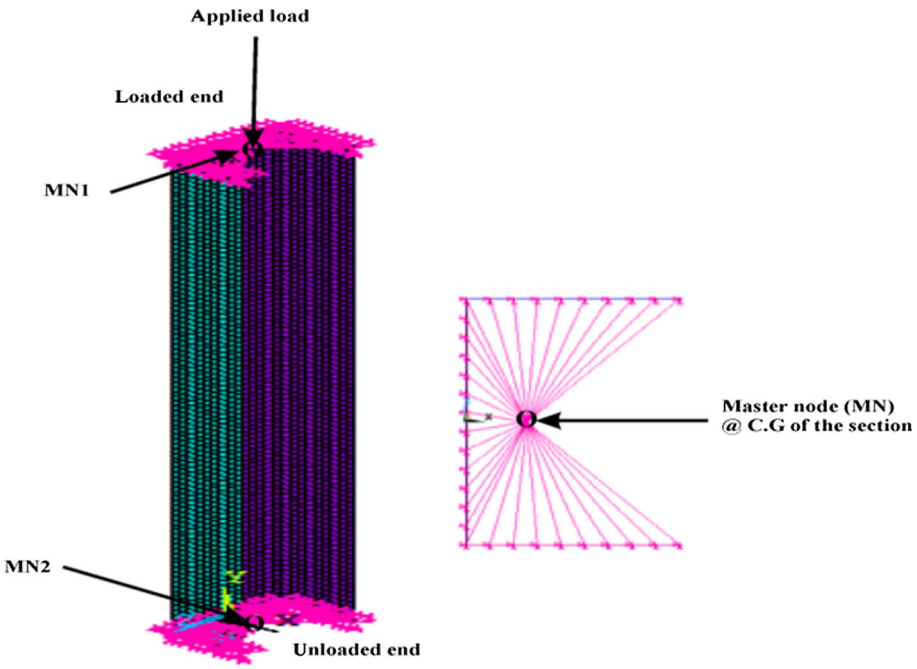

Fig. 5 Details of finite element model

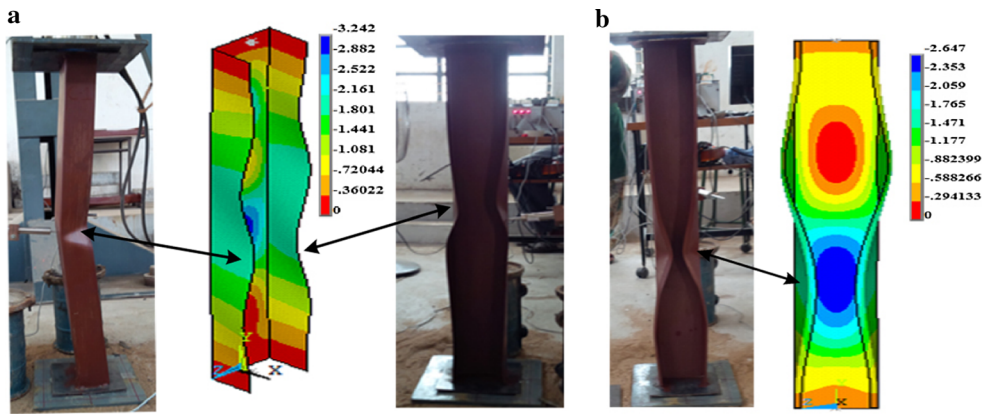

Fig. 6 Comparison of failure modes **a** SC-λ50- F270, **b** SC-I-λ50- F270

Table 3 Comparison of test and ANSYS results

S. no.	Specimen ID		Ultimate load (kN)		P_{EXP}/P_{ANSYS}	Mode of failures
			P_{EXP}	P_{ANSYS}		
1	SC	SC-λ50-F270	24.32	25.63	0.95	L
2	SC-I	SC-I-λ50-F270	61.90	71.16	0.87	L+D
3	SC-U1	SC-U-λ30-F270	70.60	72.30	0.98	L
4	SC-U2	SC-U-λ40-F270	67.80	71.37	0.95	L
5	SC-U3	SC-U-λ50-F270	64.70	71.36	0.91	L+D
6	SC-C	SC-C1-λ50-F270	70.67	72.49	0.97	L+FB
Mean					0.94	
SD					0.04	

L local buckling, *D* distortional buckling, *FT* flexural–torsional buckling, *FB* flexural buckling

section. The CG of the section is formed as master node (MN) of the FE model at the loaded (MN1) and unloaded (MN2) as shown in Fig. 5. For the uniform distribution of load over the entire cross section, a rigid region is formed via master node at the loaded (MN1) and unloaded end (MN2) of the model as shown in Fig. 5. The preliminary geometrical imperfection shape plays a critical function in the nonlinear analysis of cold-formed steel column, as its preference may adjust noticeably the corresponding buckling behaviour and ultimate strength.

First, the eigenvalue buckling analysis is performed using the geometry of the perfect member, to identify the possible buckling modes. Following this, nonlinear analysis is performed on the same model, considering both the material and geometric nonlinearities. The material behaviour of the section is described by a bilinear stress–strain curve. The geometric imperfections are included in the FEM by using a eigenvalue buckling analysis. The imperfections shape corresponding to the first buckling mode is applied using the imperfection option in ANSYS, with a scaling factor of maximum amplitude of the measured imperfection in case of Schafer and Pekoz [22]. The maximum amplitude of imperfections of 1 time the thickness for the local and distortional buckling and L/1000 for the overall buckling modes from the eigenvalue buckling analysis, is applied in the nonlinear analysis model. Finally, the nonlinear analysis is performed to obtain the ultimate load and failure modes of the sections by incorporating both geometric and material imperfections.

4 Results and Discussion

For an example, typical failure modes of the columns are shown in Fig. 6. Similar results are obtained for all the columns, and results are tabulated in Table 3. All the columns are having an equal cross-sectional area. There are three different kinds of failure modes observed, i.e. local, interactive local and distortional buckling and interactive local and overall buckling. Columns SC, SC-U1 and SC-U2 sections fail by local buckling.

Local and distortional interactive buckling is observed for the SC-I and SC-U3 section. The distortional deformation mostly occurred at the mid-height of the columns. For SC section fails by local buckling, i.e. several buckling half waves appeared along the length of the specimen (Fig. 6a). For SC-I (Fig. 6b) and SC-U3 sections, there is inward distortional buckling occurred at the mid-length of the specimen. For

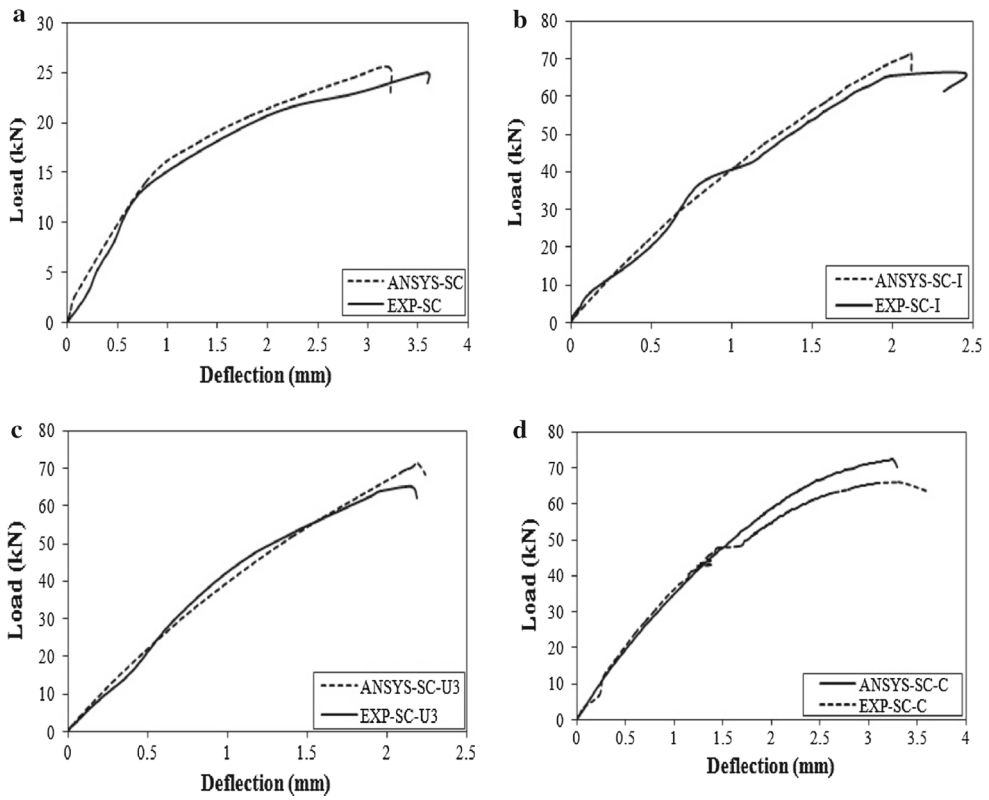

Fig. 7 Load–deflection curve **a** SC, **b** SC-I, **c** SC-U3, **d** SC-C

SC-C section fails by interaction between local and overall buckling, the local buckling half wave is observed on the flanges and maximum deformation appeared at the mid-height of the column, with the presence of complex stiffener on the flanges.

The ultimate strength of the columns SC, SC-I, SC-U3 and SC-C is 24.32, 61.90, 64.70 and 70.67 kN respectively. It is indicated that edge stiffeners have increased the torsional rigidity of the section and improve the structural performances from local buckling to flexural buckling. The strength of the section can be enhanced by adding an edge stiffener to the flange in the section SC. However, the optimized, simple channel column with complex edge stiffener (SC-C) shows the ultimate capacity is more than 66% when compared to simple channel column (SC). Typical load versus axial displacement curves are illustrated in Fig. 7. Comparisons of results between experiment (P_{EXP}) and FE analysis (P_{ANSYS}) are presented in Table 3. The average and standard deviation of P_{EXP}/P_{ANSYS} are 0.94 and 0.04 respectively. The results indicate that the proposed FE model predicts the ultimate strength of the column with a high degree of precision and reliability. From the results, it is concluded that the developed FE model is more suitable for the parametric analysis.

5 Parametric Studies

Totally, the 56 models are analysed using the developed FE model. In this parametric study, the effect of variations of thickness, yield stress and overall slenderness are analysed, and results are discussed in the subsequent sections.

5.1 Effect of Thickness Variation

In this parametric study, all the columns have a slenderness ratio is 50 and with a yield stresses of 270 N/mm^2. The effect of variation of thickness and the comparison of results between ultimate load obtained from FE analysis (P_{ANSYS}) and direct strength method ($P_{n,\,DSM}$) are presented in Table 4. In this study, three plate thicknesses (1.6, 2 and 3 mm) are considered. From this parametric study, it is observed that the thickness of the section has a significant role in the strength of the section. Rapidly, load carrying capacity of the section increases with increases in the thickness of the section.

5.2 Effect of Overall Slenderness Variation

From the test results, it is observed that the simple channel column with complex edge stiffener (SC-C) provides a better performance compared to all other sections. Hence,

Table 4 Effect of thickness variation

S. no.	Specimen ID	Section dimension (mm)					Ultimate load (kN)		$P_{ANSYS}/P_{n,DSM}$
		d	$b1$	$d1$	$d2$	t	P_{ANSYS}	$P_{n,DSM}$	
1	SC-λ50-F270-T1.6	130	85	–	–	1.6	25.63	30.02	0.85
2	SC-λ50-F270-T2.0	130	85	–	–	2	48.83	49.30	0.99
3	SC-λ50-F270-T3.0	130	85	–	–	3	107.2	169.01	0.63
4	SC-I-λ50-F270-T1.6	130	70	15	–	1.6	71.16	78.07	0.91
5	SC-I-λ50-F270-T2.0	130	70	15	–	2	92.15	112.68	0.82
6	SC-I-λ50-F270-T3.0	130	70	15	–	3	163.46	199.26	0.82
7	SC-U-λ50-F270-T1.6	130	70	15	–	1.6	71.36	90.92	0.78
8	SC-U-λ50-F270-T2.0	130	70	15	–	2	107.74	125.1	0.86
9	SC-U-λ50-F270-T3.0	130	70	15	–	3	175.77	207.2	0.85
10	SC-C1-λ50-F270-T1.6	130	55	15	15	1.6	72.49	94.35	0.77
11	SC-C1-λ50-F270-T2.0	130	55	15	15	2	99.75	138.93	0.72
12	SC-C1-λ50-F270-T3.0	130	55	15	15	3	155.78	204.21	0.76
Mean									0.81
SD									0.09

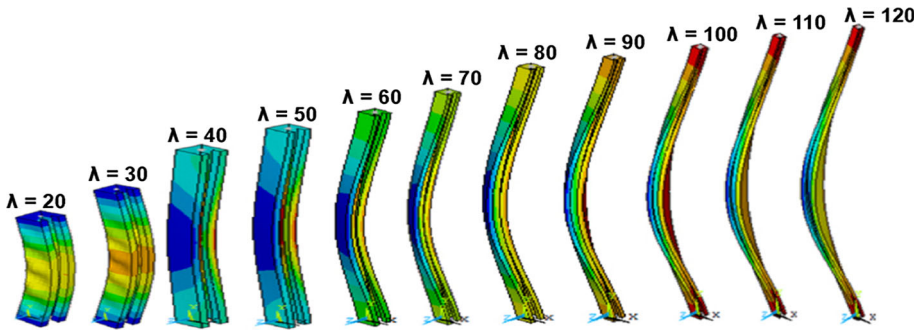

Fig. 8 Failure modes—SC-C2-λ-F270 series

a detailed parametric study is carried out on the behaviour of simple channel columns with complex edge stiffener. The dimensions of the selected cross section are met with the square (SC-C2) and rectangular (SC-C3) shapes. Two sets of cross-sectional dimensions with three yield stress of 270, 350 and 550 N/mm^2 and 12 overall slenderness variations gave 44 cross sections. The section geometry and dimensions are shown in Fig. 1d and Table 1 respectively. For each cross section, slenderness ratio (λ) varies from 20 to 120 with an increment of 10. All the specimens are failed by interactive failure mode.

As an illustration, the deformed shape at failure load and effect of yield stress variation of SC-C2-20 series of column are shown in Figs. 8 and 9 respectively. Similarly, Fig. 10 illustrates the load versus axial deformation curves for SC-C2 series of columns. For the SC-C2 column series, slenderness ratio is less than 30, the specimens failed by combining local (L), distortional (D) and flexural (F) mode, whereas the slenderness ratio is greater than 30, the specimens failed by combining distortional (D) and flexural (F) mode. However, the SC-C3 series specimens were failed by interactive failure

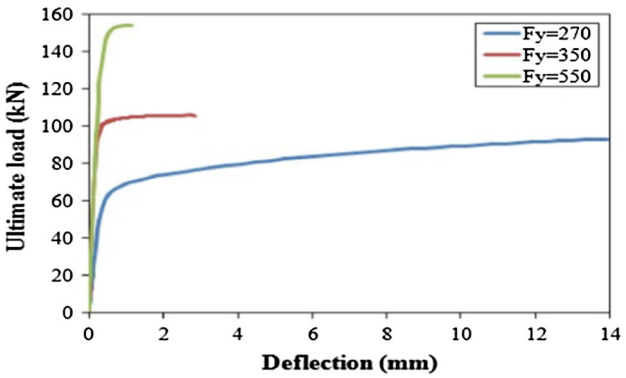

Fig. 9 Load–deflection curve for yield stress variation of SC-C2-20 series

mode. The slenderness ratio is less than 50, all the specimens failed by combining local (L) and distortional (D) buckling, whereas the slenderness ratio is greater than 50, the specimens failed by combining local (L) and flexural (F) mode. From this parametric study, it is clearly observed that the type of cross section, the magnitude of yield stress and over-

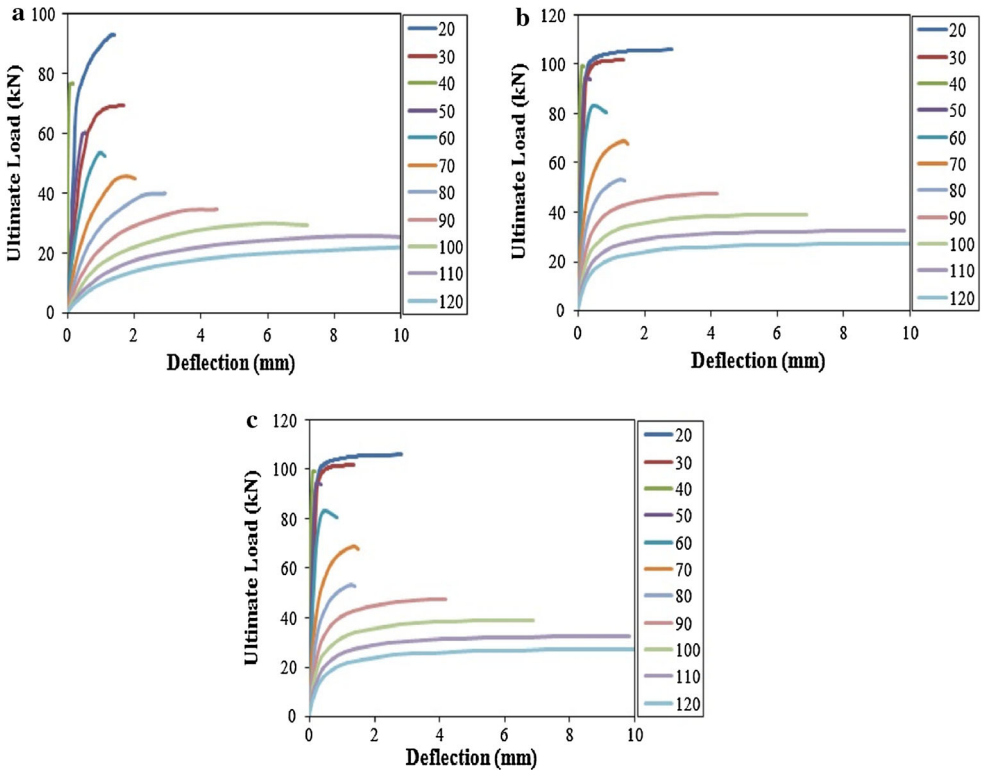

Fig. 10 Load–deflection curve for **a** SC-C2-λ -F270, **b** SC-C2-λ -F350, **c** SC-C2-λ -F550

Table 5 Comparison of results

S. no.	Specimen ID	Ultimate load (kN)		$P_{ANSYS}/P_{n,DSM}$	$P_{ANSYS}/P_{d,DSM}$	$P_{ANSYS}/P_{n,ANB}$	$P_{ANSYS}/P_{n,Pro}$	Mode of failures
		P_{ANSYS}	$P_{n,DSM}$					
1	SC-C2-20-F270	87.28	81.69	1.07	1.26	1.28	1.10	L+D+FT
2	SC-C2-30-F270	68.45	78.31	0.87	1.03	1.05	0.90	L+D+FT
3	SC-C2-40-F270	65.92	73.86	0.89	1.05	1.07	0.92	D+FT
4	SC-C2-50-F270	60.18	68.56	0.88	1.03	1.05	0.91	D+FT
5	SC-C2-60-F270	53.05	62.34	0.85	1.00	1.02	0.88	D+FT
6	SC-C2-70-F270	45.73	55.78	0.82	0.96	0.98	0.85	D+FT
7	SC-C2-80-F270	39.8	50.14	0.79	0.93	0.95	0.82	D+FT
8	SC-C2-90-F270	34.46	44.25	0.78	0.92	0.93	0.80	D+FT
9	SC-C2-100-F270	29.64	38.00	0.78	0.92	0.93	0.81	D+FT
10	SC-C2-110-F270	25.49	32.14	0.79	0.93	0.95	0.82	D+FT
11	SC-C2-120-F270	22.09	27.15	0.81	0.96	0.97	0.84	D+FT
12	SC-C2-20-F350	105.86	106.56	0.99	1.17	1.19	1.03	L+D+FT
13	SC-C2-30-F350	101.61	101.88	1.00	1.17	1.19	1.03	L+D+FT
14	SC-C2-40-F350	99.16	93.94	1.06	1.24	1.26	1.09	D+FT
15	SC-C2-50-F350	94.00	85.59	1.10	1.29	1.31	1.13	D+FT
16	SC-C2-60-F350	83.06	76.03	1.09	1.29	1.31	1.13	D+FT
17	SC-C2-70-F350	68.78	66.17	1.04	1.22	1.24	1.07	D+FT
18	SC-C2-80-F350	53.29	57.94	0.92	1.08	1.10	0.95	D+FT
19	SC-C2-90-F350	47.52	49.63	0.96	1.13	1.15	0.99	D+FT
20	SC-C2-100- F350	39.00	41.00	0.95	1.12	1.14	0.98	D+FT
21	SC-C2-110-F350	32.45	33.98	0.95	1.12	1.14	0.99	D+FT
22	SC-C2-120-F350	27.381	28.67	0.96	1.12	1.14	0.99	D+FT

Table 5 continued

S. no.	Specimen ID	Ultimate load (kN)		$P_{ANSYS}/P_{n,DSM}$	$P_{ANSYS}/P_{d,DSM}$	$P_{ANSYS}/P_{n,ANB}$	$P_{ANSYS}/P_{n,Pro}$	Mode of failures
		P_{ANSYS}	$P_{n,DSM}$					
23	SC-C2-20-F550	154.35	165.64	0.93	1.10	1.11	0.96	L+FT
24	SC-C2-30-F550	150.97	151.55	1.00	1.17	1.19	1.03	D+FT
25	SC-C2-40-F550	137.06	133.97	1.02	1.20	1.22	1.06	D+FT
26	SC-C2-50-F550	115.00	114.53	1.00	1.18	1.20	1.04	D+FT
27	SC-C2-60-F550	89.56	93.77	0.96	1.12	1.14	0.99	D+FT
28	SC-C2-70-F550	69.49	74.19	0.94	1.10	1.12	0.97	D+FT
29	SC-C2-80-F550	56.56	59.41	0.95	1.12	1.14	0.98	D+FT
30	SC-C2-90-F550	46.2	47.94	0.96	1.13	1.15	1.00	D+FT
31	SC-C2-100-F550	36.23	38.81	0.93	1.10	1.12	0.96	D+FT
32	SC-C2-110-F550	31.15	32.14	0.97	1.14	1.16	1.00	D+FT
33	SC-C2-120-F550	26.22	27.15	0.97	1.14	1.16	1.00	D+FT
34	SC-C3-20-F270	88.91	78.28	1.14	1.34	1.36	1.17	L+DB
35	SC-C3-30-F270	68.36	76.24	0.90	1.05	1.07	0.93	L+DB
36	SC-C3-40-F270	65.70	73.26	0.90	1.06	1.07	0.93	L+DB
37	SC-C3-50-F270	64.48	69.88	0.92	1.09	1.10	0.95	L+DB
38	SC-C3-60-F270	58.07	66.01	0.88	1.03	1.05	0.91	L+FB
39	SC-C3-70-F270	52.85	61.52	0.86	1.01	1.03	0.89	L+FB
40	SC-C3-80-F270	53.94	57.33	0.94	1.11	1.13	0.97	L+FB
41	SC-C3-90-F270	48.00	53.02	0.91	1.07	1.08	0.94	L+FTB
42	SC-C3-100-F270	46.67	47.86	0.98	1.15	1.17	1.01	L+FTB
43	SC-C3-110-F270	44.51	43.10	1.03	1.21	1.24	1.07	L+FTB
44	SC-C3-120-F270	42.35	38.74	1.09	1.29	1.31	1.13	L+FTB
Mean				0.94	1.11	1.13	0.97	
SD				0.13	0.10	0.11	0.09	

L local buckling, *D* distortional buckling, *FT* flexural–torsional buckling, *FB* flexural buckling

all slenderness ratio is significantly affecting the strength and behaviour of the column.

6 Theoretical Investigations

Based on the direct strength method (DSM), the nominal capacity of members in axial compression ($P_{n,DSM}$) shall be minimum of local buckling (P_{nl}), distortional buckling (P_{nd}) and flexural–torsional buckling (P_{ne}).

$$P\text{ne} = \begin{cases} (0.658)^{\lambda c^2} P_y & \text{for } \lambda_c \le 1.5 \\ \left(\frac{0.877}{\lambda c^2}\right) P_y & \text{for } \lambda_c > 1.5 \end{cases} \quad (1)$$

where $\lambda_c = \sqrt{P_y/P_{cre}}$ and $P_y = Af_y.P_y$ is the squash load.

The nominal axial strength (P_{nl}) for local buckling is

$$P_{nl} = \begin{cases} P_{ne} & \text{for } \lambda_1 \le 0.776 \\ \left(1 - 0.15\left(\frac{P_{crl}}{P_{ne}}\right)^{0.4}\right)\left(\frac{P_{crl}}{P_{ne}}\right) P_{ne} & \text{for } \lambda_1 > 0.776 \end{cases} \quad (2)$$

where $\lambda_1 = \sqrt{P_{ne}/P_{crl}}$.

The nominal axial strength (P_{nd}) for distortional buckling is

$$P_{nd} = \begin{cases} P_y & \text{for } \lambda_d \le 0.561 \\ \left(1 - 0.25\left(\frac{P_{crd}}{P_y}\right)^{0.6}\right)\left(\frac{P_{crd}}{P_y}\right)^{0.6} P_y & \text{for } \lambda_d > 0.561 \end{cases} \quad (3)$$

where $\lambda_d = \sqrt{P_y/P_{crd}}$.

The critical elastic local load P_{crl} and distortional buckling load P_{crd} are computed using linear elastic finite strip buckling analysis. Three dissimilar approaches are used to estimate the ultimate strength of the simple channel column with complex edge stiffener. In the first DSM approach, the nominal ultimate strength of the section ($P_{n,DSM}$) is equal to the least of (P_{ne}, P_{nl}, P_{nd}). In the second DSM approach, the design ultimate strength of the section ($P_{d,DSM}$) is equal to the 0.85 times the least of (P_{ne}, P_{nl}, P_{nd}). In the third approach, nominal resistance of the section is estimated by using a modification factor proposed by $P_{n,ANB}$ [23], which

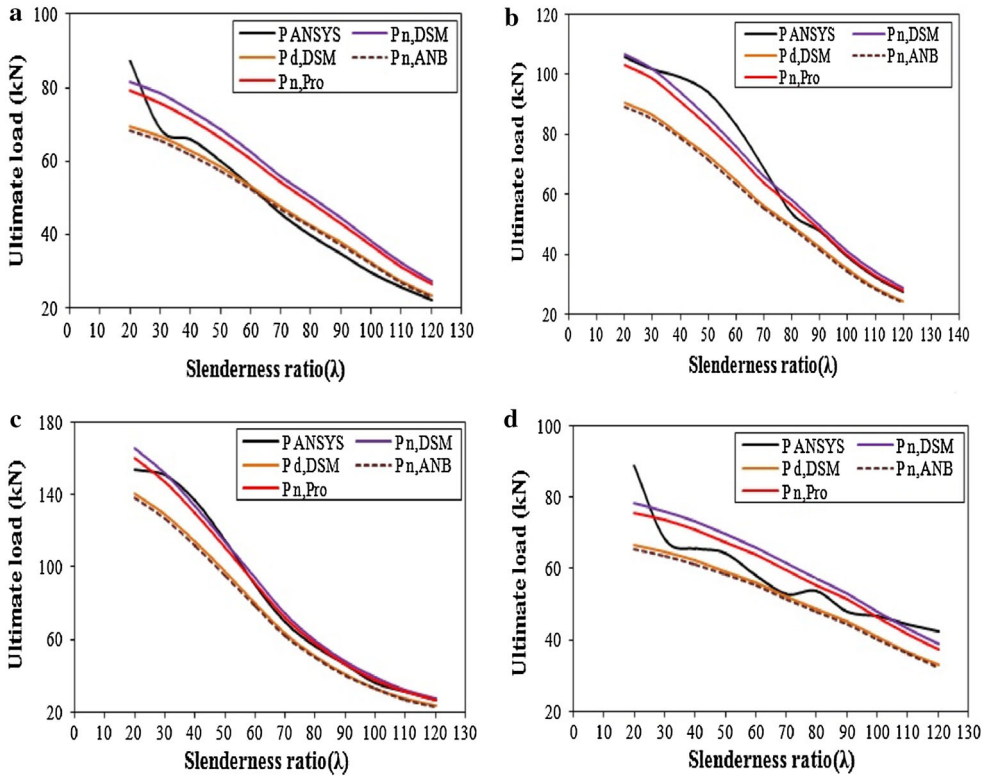

Fig. 11 Comparison of results **a** SC-C2-λ -F270 **b** SC-C2-λ -F350 **c** SC-C2-λ -F550 **d** SC-C3-λ -F270

is equal to the 0.836 times the least of ($P_{ne,}$ $P_{nl,}$ P_{nd}). However, to obtain exact resistance of the simple channel column with complex edge stiffener, a new design expression is proposed ($P_{n,Pro}$). The comparison of results between the FEA and various design standards is discussed in Table 5 and Fig. 11.

Except for the SC-C3-λ-F550 series of column, the direct strength method ($P_{n,\,DSM}$) is producing unconservative results. The strength obtained from the $P_{d,\,DSM}$ and $P_{n,\,ANB}$ approach predicts unconservative results for the SC-C2-λ-F350 and SC-C2-λ-F550 series of column. The mean and standard deviation of $P_{ANSYS}/P_{n,\,DSM}$ are 0.94 and 0.13, the mean and standard deviation of $P_{ANSYS}/P_{d,\,DSM}$ are 1.11 and 0.10 and the mean and standard deviation of $P_{ANSYS}/P_{n,\,ANB}$ are 1.13 and 0.11, respectively.

However to predict the accurate results, a new design modification factor is proposed in this study. A linear regression analysis is conducted between P_{ANSYS} and $P_{n,\,DSM}$ as shown in Fig. 12. The relationship between the ultimate capacity predicted by finite element analysis (P_{ANSYS}) and the direct strength method ($P_{d,\,DSM}$) is almost linear as $P_{n,\,pro} = 0.968^{*}\ P_{n,\,DSM}$. The mean and standard deviation of $P_{ANSYS}/P_{n,\,pro}$ are 0.97 and 0.09, respectively. The proposed design equation is also verified by the results available from the literature (18), and the results are displayed in Table 6. The corresponding mean and standard deviation of

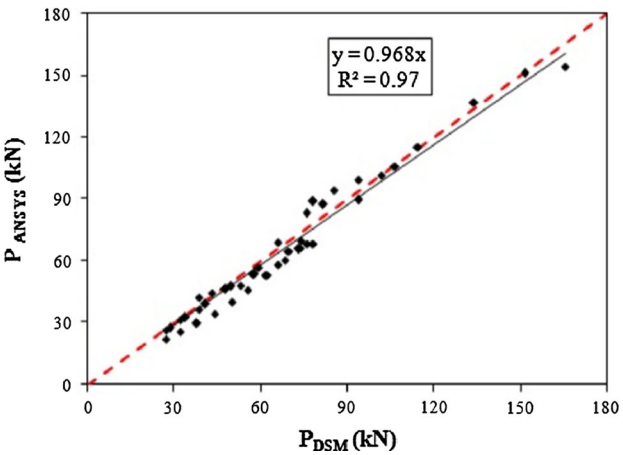

Fig. 12 Relationship between ANSYS and DSM results

$P_{EXP}/P_{n,\,Pro}$ are 1.01 and 0.02, respectively. From the test results, it is observed that the proposed design equation moderately predicts the strength of the simple channel column with complex edge stiffener.

7 Summary and Conclusions

An experimental and numerical investigation of the structural behaviour of pinned-ended simple cold-formed steel chan-

Table 6 Comparison of proposed model with test results from literature [18]

Specimen ID as per literature	Load (kN)			$P_{EXP}/P_{n,Pro}$
	P_{EXP}	P_{DSM}	$P_{n,Pro}$	
T1.5F120L0500	168.90	164.70	163.60	1.03
T1.5F120L3000	131.30	133.30	131.61	1.00
T1.5F120L3500	127.40	123.20	121.31	1.05
T1.9F120L0500	233.70	234.2	234.42	1.00
T1.9F120L1000	231.20	230.8	230.96	1.00
T1.9F120L1500	227.30	225.1	225.15	1.01
Mean				1.01
SD				0.02

nel column with various types of edge stiffener is discussed. Totally, six columns are tested experimentally, and the results are verified by using developed finite element modelling, and good correlation is achieved. The effect of variations of thickness, yield stress and overall slenderness are analysed by using the developed FE model. The strength of the sections obtained from the finite element analysis is compared with the direct strength method specifications for the cold-formed steel structures. The subsequent conclusions are drawn from these investigations.

- All the slenderness range of the column, global buckling is observed in premature stage of analysing and followed by the local and distortional buckling is observed in the later stage of testing.
- The current DSM ($P_{n,DSM}$) approaches overestimated the strength of the section. It confirms the inadequacy of the current DSM specifications in predicting the ultimate strength of the column experiencing in overall buckling interaction.
- In addition, it is found that the $P_{n,DSM}$ and $P_{d,DSM}$ approaches provide overestimated results, whereas the $P_{n,ANB}$ and $P_{n,pro}$ approaches predict the underanticipated results in the column with grade of steel that is equal to 270 N/mm^2. However, $P_{n,ANB}$ and $P_{n,pro}$ approaches estimate to some extent unsafe and exhibit the speckled results.
- Similarly, $P_{n,ANB}$ and $P_{d,DSM}$ approaches provide underestimated results for all the slenderness ranges of the column, whereas $P_{n,DSM}$ and $P_{n,pro}$ approaches estimate slightly unsafe for the intermediate overall slenderness (λ) range of the column (30–90) with grade of steel that is equal to 350 N/mm^2. However, the proposed design approach ($P_{n,pro}$) estimates safe and reliable results in all slenderness ranges of the column.
- It is also observed that $P_{n,ANB}$ and $P_{d,DSM}$ approaches provide underestimated results for all the slenderness ranges of the column, whereas $P_{n,DSM}$, and $P_{n,pro}$ approaches estimate safe and reliable results in all slenderness ranges of the column with grade of steel that is equal to 550 N/mm^2.
- The proposed design approach ($P_{n,pro}$) estimates safe and reliable results in all the aspects of the column with the mean and standard deviation of 0.97 and 0.09, respectively.

References

1. Wang, C.; Zhang, Z.; Zhao, D.; Liu, Q.: Compression tests and numerical analysis of web-stiffened channels with complex edge stiffeners. J. Constr. Steel Res. **116**, 29–39 (2016)
2. Batista, E.M.: Buckling curve for cold-formed compressed members. J. Constr. Steel Res. **28**, 121–136 (1994)
3. Young, B.; Rasmussen, J.R.: Design of lipped channel columns. J. Struct. Eng. **124**, 140–148 (1998)
4. Young, B.; Hancock, G.J.: Compression tests of channels with inclined simple edge stiffeners. J. Struct. Eng. **129**, 1403–1411 (2003)
5. Young, B.: Design of channel columns with inclined edge stiffeners. J. Constr. Steel Res. **60**, 183–197 (2004)
6. Anil Kumar, M.V.; Kalyanaraman, V.: Design strength of locally buckling stub-lipped channel columns. J. Struct. Eng. **138**, 1291–1299 (2012)
7. Ungermann, D.; Lubke, S.; Brune, B.: Tests and design approach for plain channels in local and coupled local-flexural buckling based on eurocode3. Thin-Walled Struct. **81**, 108–120 (2014)
8. Ananthi, G.B.; Palani, G.S.; Iyer, N.R.: Numerical and theoretical studies on cold-formed steel unlipped channels subjected to axial compression. Lat. Am. J Solids Struct. **12**, 1–17 (2015)
9. Young, B.; Yan, J.: Design of cold-formed steel channel columns with complex edge stiffeners by direct strength method. J. Struct. Eng. **130**, 1756–1763 (2002)
10. Becque, J.; Rasmussen, K.J.R.: Experimental investigation of local-overall interaction buckling of stainless steel lipped channel columns. J. Constr. Steel Res. **65**, 1677–1684 (2009)
11. Silvestre, N.; Camotim, D.; Dinis, P.B.: Direct strength prediction of lipped channel columns experiencing local-plate/distortional interaction. Adv. Steel Const. **5**, 49–71 (2009)
12. Dinis, P.B.; Camotim, D.; Batista, E.M.; Santos, E.: Local/distortional/global mode coupling in fixed lipped channel columns: behaviour and strength. Adv. Steel Const. **7**, 113–130 (2011)
13. Silvestre, N.; Camotim, D.; Dinis, P.B.: Post-buckling behaviour and direct strength design of lied channel columns experiencing local/distortional interaction. J. Constr. Steel Res. **73**, 12–30 (2012)

14. Loughlan, J.; Yidris, N.; Jones, K.: The failure of thin-walled lied channel compression members due to coupled local-distortional interactions and material yielding. Thin-Walled Struct. **6**, 14–21 (2012)
15. Schafer, B.W.; Peköz, T.: Direct strength prediction of cold formed steel members using numerical elastic buckling solutions. In: Proceedings of 14th International Specialty Conference on Cold-Formed Steel Structures, Univ. of Missouri-Rolla, Rolla, pp, 69–76 (1998)
16. Schafer, B.W.: Local, distortional, and Euler buckling of thin-walled columns. J. Struct. Eng. **128**, 289–299 (2002a)
17. Schafer, B.W.: Progress on the direct strength method. In: Proceedings of 16th International Specialty Conference on Cold-Formed Steel Structures, Orlando, pp. 647–662 (2002b)
18. Yan, J.; Young, B.: Column tests of cold-formed steel channels with complex stiffeners. J. Struct. Eng. **128**, 737–745 (2002)
19. Sukumar, S.; Parameswaran, P.; Jayagopal, L.S.: Local distortional and Euler-buckling of thin walled built-up open sections under compression. J. Struct. Eng. SERC India **32**, 54–447 (2006)
20. Manikandan, P.; Arun, N.: Behaviour of partially closed stiffened cold-formed steel compression member. Arab. J. Sci. Eng. **41**, 3865–3875 (2016)
21. Salem, A.H.; El Aghoury, M.A.; Hassan, S.K.; Amin, A.A.: Post-buckling strength of battened columns built from cold-formed lipped channels. Emir. J. Eng. Resc. **9**(2), 117–125 (2004)
22. Schafer, B.; Pekoz, T.: Computational modelling of cold-formed steel: characterizing geometrical imperfections and residual stresses. J. Constr. Steel Res. **47**, 193–210 (1998)
23. Anbarasu, M.; Sukumar, S.: Local/distortional/global buckling mode interaction on thin walled lied channel columns. Lat. Am. J. Solids Struct. **11**, 1363–1375 (2014)
24. ENV 1993-1-4:2006/AC.: European pre-standard design of steel structures-part 1-3:General rules—supplementary rules for cold formed thin gauge members and sheeting